

# Kinetics and Mechanism of the Complex Oxidation of Aminoiminomethanesulfonic Acid by Iodate in Acidic Medium<sup>1</sup>

Elizabeth Mambo and Reuben H. Simoyi\*

Department of Chemistry, West Virginia University, Box 6045, Morgantown, West Virginia 26506-6045

Received: August 5, 1993; In Final Form: October 6, 1993\*

The reaction between iodate and aminoiminomethanesulfonic acid,  $\text{NH}_2(\text{NH})\text{CSO}_2\text{H}$  (AIMSA), has been studied in acidic medium. The stoichiometry of the reaction in excess AIMSA is  $2\text{IO}_3^- + 3\text{AIMSA} + 3\text{H}_2\text{O} \rightarrow 3\text{SO}_4^{2-} + 3\text{CO}(\text{NH}_2)_2 + 2\text{I}^- + 6\text{H}^+$  (eq 1), and the stoichiometry of the reaction in excess iodate is  $4\text{IO}_3^- + 5\text{AIMSA} + 3\text{H}_2\text{O} \rightarrow 5\text{SO}_4^{2-} + 5\text{CO}(\text{NH}_2)_2 + 2\text{I}_2 + 6\text{H}^+$  (eq 2). In excess AIMSA and high acid concentrations the reaction shows an induction period and a transient formation of iodine, while in excess iodate concentrations iodine is produced and partially consumed, leaving a finite iodine concentration at the end of the reaction. The dynamics of the reaction is explained by a combination of three reactions: the first is the oxidation of AIMSA by iodate to give iodide, the second is the Dushman reaction which forms iodine from the iodate-iodide reaction, and the third is the reaction of iodine and AIMSA. The relative rates of these three reactions will determine the dynamics of the reaction. The oxidation of AIMSA with  $\text{I}_2$  and  $\text{I}_3^-$  was also investigated. The oxidation of AIMSA by  $\text{I}_2$  and  $\text{I}_3^-$  was found to be inhibited by acid because the oxidation of AIMSA by  $\text{HOI}$  is faster than that with molecular  $\text{I}_2$ . The reaction is also autoinhibitory because the product of the reaction,  $\text{I}^-$ , combines with unreacted  $\text{I}_2$  to form  $\text{I}_3^-$  which is relatively inert toward AIMSA. A computer simulation study is performed to enhance the proposed mechanism.

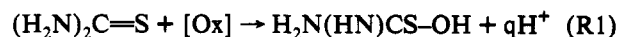
## Introduction

Nonlinear dynamics in chemistry is dominated by oxyhalogen compounds and sulfur-based compounds.<sup>2</sup> Sulfur compounds have only been recently included as a source of nonlinear dynamics in chemical systems.<sup>3</sup> While the chemistry and thermodynamics of oxyhalogen compounds are widely known, very little is known about sulfur chemistry. The lack of information on sulfur chemistry has stalled any further studies on nonlinear phenomena in chemistry.

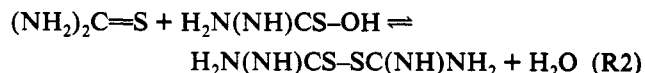
The importance of sulfur chemistry now spills into environmental issues since the major source of pollutants in coal-fired industrial applications is sulfur oxides which subsequently contribute to acid rain.<sup>4</sup> The problem is to understand the chemistry of sulfur well enough to enable the conversion of these toxic sulfur compounds into innocuous versions. In the field of nonlinear dynamics, sulfur compounds are heavily implicated in chemical oscillations,<sup>5-8</sup> clock and crazy clock reactions,<sup>9</sup> chemical waves,<sup>10</sup> and spatial patterns.<sup>11</sup> The rate of discovery of various nonlinear dynamics in chemistry and physics based on sulfur chemistry has proceeded at a pace that outgrew the basic knowledge available on sulfur compounds.<sup>12</sup> The kinetics parameters, especially, which are of relevance to our understanding the basis of nonlinear phenomena in chemistry are the least understood.

We have recently embarked on a systematic study of the kinetics and mechanisms of sulfur-based reactions that are of relevance to some nonlinearity we wish to study.<sup>13</sup> For example, the discovery of a traveling wave in chlorite-thiourea mixtures prompted us to study in detail the kinetics and mechanism of the fundamental "drive" reaction.<sup>14</sup> The study of kinetics and mechanism of sulfur reactions is, however, very complex due to such features as autocatalysis,<sup>15</sup> autoinhibition,<sup>16</sup> free radical mechanisms,<sup>17,18</sup> polymerizations,<sup>19</sup> oligooscillations,<sup>20</sup> variable stoichiometries,<sup>21</sup> and wide pH ranges over which the reactions are viable.<sup>22</sup> No complete kinetics study of the oxidation of a sulfur compound that has been done so far has not involved at least one of these nonlinearities.

Earlier studies of the oxidation of thiourea by iodate<sup>16</sup> and by chlorite<sup>14</sup> postulated successive oxygen additions on the sulfur atom with a cleavage of the sulfur-carbon bond when the sulfur attains the sulfonic acid oxidation state ( $-\text{SO}_3\text{H}$ ). The rate-determining step had been suggested to be the formation of the sulfenyl acid:



The sulfenyl acid then proceeds successively through the sulfinic acid and the sulfonic acid and then to sulfate. The proof of this assertion (pH measurements, redox potentials) was marred by the fact that the sulfenyl acid rapidly dimerizes in the presence of a mild oxidizing agent (e.g.,  $\text{I}_2$ )<sup>16,20</sup> or in the absence of further oxidant (e.g., stoichiometric deficiency of the oxidant):<sup>16</sup>



Other possibilities of thiosulfonates also exist.<sup>23</sup>

We report in this paper a comprehensive kinetics and mechanistic study of the reaction of iodate with aminoiminomethanesulfonic acid,  $\text{NH}_2(\text{NH})\text{CSO}_2\text{H}$  (AIMSA). This kinetics study was performed as a way of conclusively deciphering the oxidation mechanism of thiourea and other general sulfur compounds of this nature. Our previous studies postulated AIMSA to be one of the intermediates generated in the oxidation pathway of thiourea to sulfate.<sup>14</sup> AIMSA was chosen because it is stable enough to be isolated in crystalline form, and it does not polymerize in aqueous environments.<sup>24</sup> The sulfur atom in AIMSA is at the +2 oxidation state which lies between the -2 oxidation state in thiourea and the +6 state in sulfate. Coupled with this kinetics study is a computer simulation analysis of our proposed mechanism.

## Experimental Section

**Materials.** (Eastman Kodak), sodium perchlorate, potassium iodate, potassium iodide, soluble starch, sodium thiosulfate, perchloric acid 72% (Fisher), hydrochloric acid, and sodium carbonate (J.T. Baker) were used as purchased. All solutions

\* Abstract published in *Advance ACS Abstracts*, November 15, 1993.

were prepared using singly distilled water. AIMSAs solutions were prepared just before use and not kept for more than 4 h. Aqueous solutions of AIMSAs gave out a hydrogen sulfide odor a short while after preparation or after being warmed.

**Methods.** All experiments were carried out at a constant ionic strength of 0.5 M (sodium perchlorate). Perchloric acid, AIMSAs, and sodium perchlorate solutions were mixed in one vessel, and iodate solution was mixed in another vessel. The reaction was monitored spectrophotometrically at 460 nm, which is the isosbestic point of triiodide and iodine, with a Hi-Tech Scientific SF-61 stopped flow spectrophotometer with an M300 monochromator and a spectrascan control unit. The data from the spectrophotometer were amplified and digitized via an Omega Engineering DAS-50/1 16-bit A/D board and interfaced to a Tandon 386SX computer for storage. The data were analyzed for induction periods, initial rates, and maximum absorbance of iodine produced. All experiments were performed at  $25 \pm 0.1$  °C.

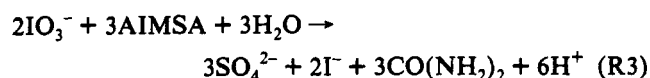
Four sets of experiments each with six runs were carried out. The first set was performed in excess iodate over AIMSAs with an acid concentration that ranged between 0.02 and 0.08 M. The second set of experiments was performed in excess iodate and high acid concentration ranging from 0.08 to 0.20 M. The third series of experiments was an acid dependence set performed in excess AIMSAs. The last series was carried out at constant AIMSAs and iodate varying from 0.002 to 0.005 M while acid was kept constant at 0.008 M.

Experiments involving the reaction between iodine and triiodide with AIMSAs were also monitored at 460 nm. The experiments were carried out in at least 5-fold excess of AIMSAs over iodine except for initial rate-determining experiments in which all ranges of concentration ratios were attempted. Triiodide was formed by adding measured amounts of potassium iodide crystals to aqueous iodine solutions.

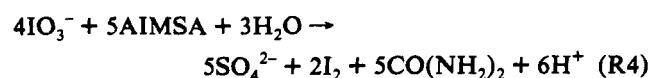
The stoichiometry of the reaction was determined in excess iodate at a pH of about 1.5. Nine sets of experiments were carried out with iodate ranging from 0.0022 to 0.004 M with AIMSAs constant at 0.005 M. All runs were left overnight. The total iodine formed plus the remaining iodate were determined iodometrically by adding excess acidified iodide and titrating with sodium thiosulfate using starch indicator. Qualitative pH changes were measured using an Orion PH meter Model 420A. Sulfate was determined gravimetrically as BaSO<sub>4</sub>. Iodide was determined gravimetrically as AgI (after removing SO<sub>4</sub><sup>2-</sup>) as well as colorimetrically using *p*-aminophenol.<sup>25</sup>

## Results

The stoichiometry of the reaction in excess AIMSAs was determined as



Approximately 97% of the sulfate expected in stoichiometry R3 was obtained as BaSO<sub>4</sub>. At the exact mole ratio of iodate to AIMSAs of 2:3 no iodine was obtained at the end of the reaction. A slight increase in iodate above the 2:3 ratio produces iodine at the end of the reaction. In excess iodate, the stoichiometry was determined as



This was determined by quantitatively monitoring SO<sub>4</sub><sup>2-</sup>, correlating I<sub>2</sub> produced with initial AIMSAs concentration, and iodometrically determining the total IO<sub>3</sub><sup>-</sup> and I<sub>2</sub> left at the end of the reaction. Table I summarizes these results.

## Reaction Dynamics

All reactions in low acid are characterized by a long induction period in which no iodine is formed. For acid concentrations of

**TABLE I: Stoichiometric Data<sup>a</sup>**

reactants		products			
[IO <sub>3</sub> <sup>-</sup> ] <sub>0</sub>	[AIMSAs] <sub>0</sub>	[I <sub>2</sub> ] <sub>f</sub>	%	[SO <sub>4</sub> <sup>2-</sup> ] <sub>f</sub>	%
0.005	0.010	0	100	0.004 65	93
0.005	0.008	0	100	0.004 7	94
0.004	0.006	0	100	0.003 88	97
0.005	0.003	0.0015	96	0.002 9	97
0.005	0.005	0.0019	96	0.004 85	97

<sup>a</sup> Reactions were run in 100-mL aliquots. Iodine was determined spectrophotometrically at 460 nm and iodometrically by titrating with S<sub>2</sub>O<sub>3</sub><sup>2-</sup>. Sulfate was determined gravimetrically as BaSO<sub>4</sub>. The symbol % relates to the calculated percentage as expected from stoichiometries R3 and R4.

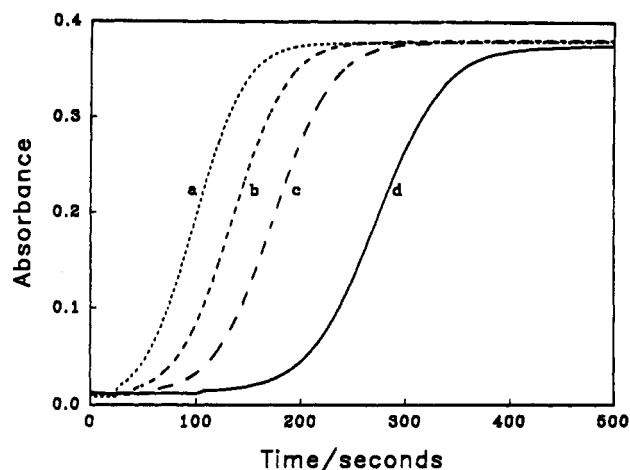


**Figure 1.** Absorbance traces ( $\lambda = 460$  nm) at the I<sub>2</sub>/I<sub>3</sub><sup>-</sup> isosbestic point. The traces show the induction period and the slow monotonic increase of [I<sub>2</sub>] in excess [IO<sub>3</sub><sup>-</sup>]. [AIMSAs]<sub>0</sub> = 0.001 25 M; [IO<sub>3</sub><sup>-</sup>]<sub>0</sub> = 0.0025 M. [H<sup>+</sup>]<sub>0</sub> = (a) 0.060, (b) 0.040, (c) 0.030, and (d) 0.020 M.

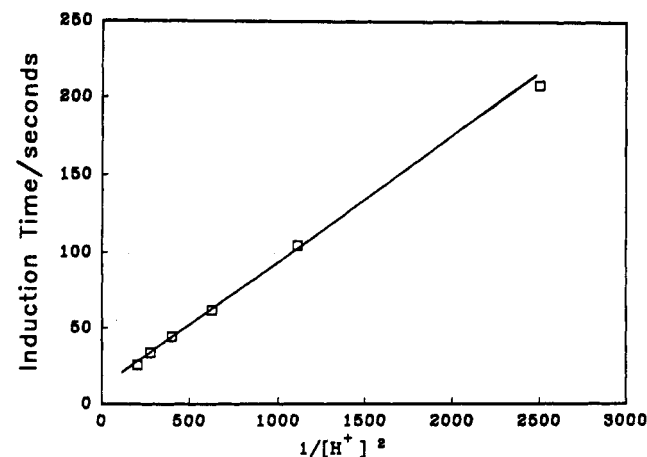


**Figure 2.** Plot of induction time against [H<sup>+</sup>]<sup>-2</sup> showing the linear dependence. [AIMSAs]<sub>0</sub> = 0.005 M, [IO<sub>3</sub><sup>-</sup>]<sub>0</sub> = 0.0025 M.

0.02–0.08 M the induction period ranges from 210 to 33 s. The induction period was effectively eliminated in acid concentrations greater than 0.10 M. In moderately low acid concentrations and excess iodate concentrations over AIMSAs, there is a monotonic increase in iodine concentrations after the induction period (Figure 1). The induction period is inversely proportional to the square of the initial acid concentration, and a plot of induction time vs 1/[H<sup>+</sup>]<sup>2</sup> is a straight line at high acid concentrations (Figure 2).

In high acid concentrations (above 0.08 M) and excess iodate concentrations, there is a negligible induction period followed by a rapid formation of iodine which attains a maximum value before falling to a finite concentration that is determined by the initial AIMSAs concentration (Figure 3). The moles of iodine produced equal 40% of the initial AIMSAs concentration. This is as predicted by stoichiometry R4. A similar trend is observed in excess AIMSAs. In this case iodine diminishes to zero, and its

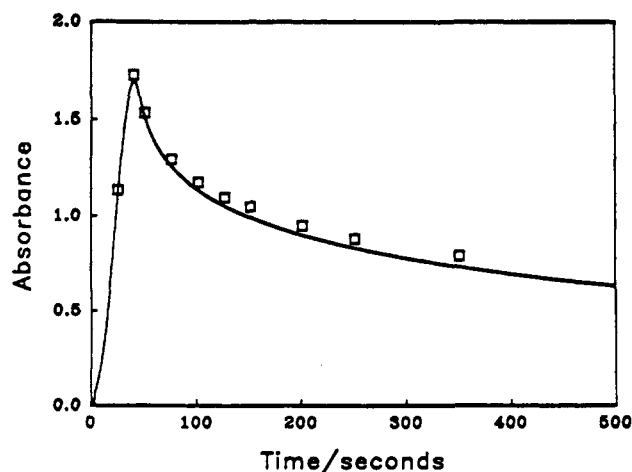


**Figure 3.** Absorbance traces in high acid and excess iodate. The data points represent simulated data from the mechanism in Table I.  $[H^+] = 0.08$  M,  $[AIMSA]_0 = 0.005$  M, and  $[IO_3^-] = 0.008$  M.

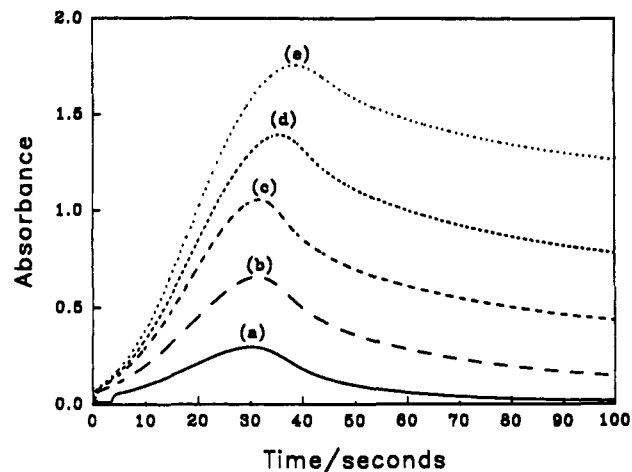


**Figure 5.** Effect of progressively increasing  $[IO_3^-]$  at constant acid and AIMSA.  $[AIMSA]_0 = 0.008$  M;  $[H^+]_0 = 0.08$  M.  $[IO_3^-]_0 =$  (a) 0.001, (b) 0.002, (c) 0.003, (d) 0.004, and (e) 0.005 M.

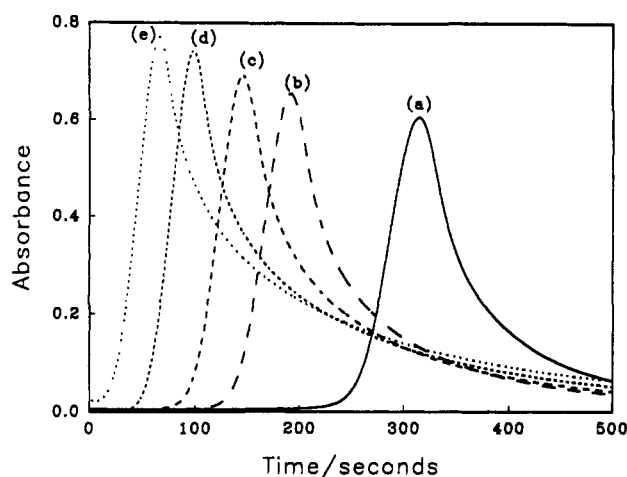


**Figure 4.** A series of traces in excess AIMSA and high acid. The effect of acid can be seen in the form of a shorter induction period and a higher maximum iodine concentration.  $[AIMSA]_0 = 0.005$  M,  $[IO_3^-] = 0.0025$  M.  $[H^+]_0 =$  (a) 0.02, (b) 0.03, (c) 0.04, (d) 0.06, and (e) 0.08 M.

consumption appears to be slower than its formation (Figure 4). Acid concentrations affect both the induction period and the maximum amount of iodine formed. A plot of the maximum iodine absorbance observed in Figure 4 against the initial acid concentration gives a direct relationship with saturation. Saturation behavior is expected since the total amount of iodine formed is limited by initial iodate concentrations. Theoretically, the maximum transient iodine concentration that can be obtained is when the  $IO_3^- \rightarrow I^-$  reaction is significantly faster than the  $I_2 \rightarrow AIMSA$  reaction. Figure 5 shows the reaction dynamics at constant  $[AIMSA]_0$  and variable  $[IO_3^-]_0$ . Maximum transient iodine produced is proportional to the initial  $IO_3^-$  concentration with a saturation value, as  $[IO_3^-]_0$  exceeds stoichiometric values, determined by reaction R4.  $IO_3^-$  controls the rate of formation of  $I_2$  but is not involved in the rate of consumption of  $I_2$ . At very low acid concentrations (circa  $10^{-3}$  M) the reaction goes to completion as determined by stoichiometry R3 without any transient formation of iodine. Figure 5 also shows the effect of iodate concentrations. At low enough iodate concentrations the iodine is completely consumed, but as the iodate increases past the stoichiometric value, a finite iodine concentration is retained at the end of the reaction.

Iodine is a very important reactant/intermediate/product in this reaction system. Addition of small amounts of iodide of about  $10 \mu\text{M}$  concentrations noticeably catalyzed the reaction, sharply reducing the induction period (by half in most instances). Addition of higher iodide concentrations distorted the maximum transient iodine concentrations obtained and completely elimi-

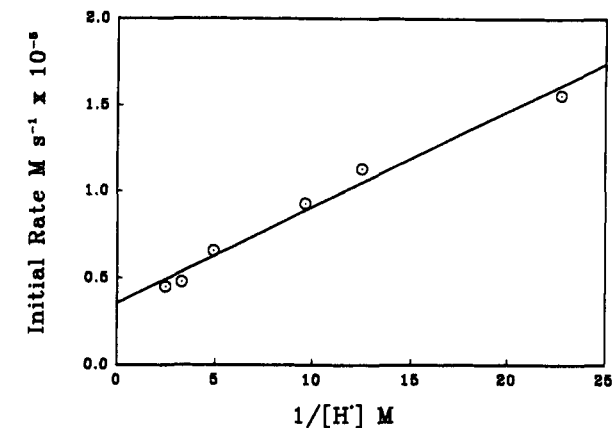
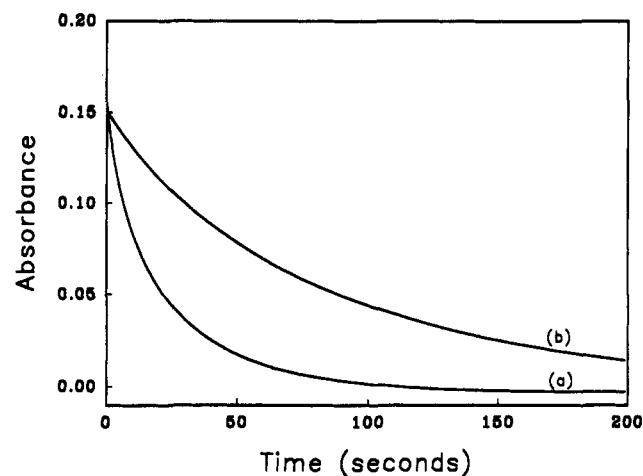


**Figure 6.** (a, top) Absorbance traces of the reaction between AIMSA and  $I_2$  and  $I_3^-$ .  $[AIMSA]_0 = 0.0025$  M,  $[I_2]_0 = 0.0002$  M, and  $[H^+]_0 = 0.044$  M. Trace a had no iodide, and trace b has 0.002 M iodide initial added. (b, bottom) Inverse acid dependence plot of the initial rate of the  $I_2$ -AIMSA reaction.  $[I_2]_0 = 0.0002$  M,  $[AIMSA]_0 = 0.0025$  M, and  $[I^-]_0 = 0.0001$  M.

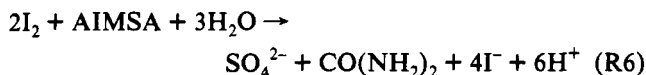
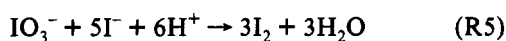
nated the induction period. In excess AIMSA conditions iodide is the normal reduction product of iodate, while in excess iodate conditions it is one of the most important intermediates. At low iodide concentrations (up to  $5 \times 10^{-5}$  M), the induction period was inversely proportional to the iodide concentration. From such a plot we estimate by extrapolation that normal iodate solutions contain  $4 \times 10^{-6}$  M iodide. This is very close to the figure of  $5 \times 10^{-6}$  M deduced from a previous study.<sup>26</sup>

**Iodine-AIMSA Reaction.** Kinetics traces were also obtained for the reaction between iodine and AIMSA. The rate of

consumption of iodine in 5–20-fold excess of AIMSAs over iodine is surprisingly slow for what would have been considered a pseudo-first-order kinetics environment. The reaction starts off quite fast and quickly slows down as in typical autoinhibitory reactions. The reaction was first order in both iodine and AIMSAs. It was inhibited by both iodide and acid. Figure 6a shows two absorbance traces that show the effect of iodide. A plot of initial rate vs  $[H^+]^{-1}$  gives a straight line with a positive intercept if iodide is initially added to the reaction mixture (Figure 6b). Without initial addition of iodide, the linear relationship is lost.

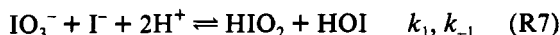
### Mechanism

The reaction dynamics suggest that there are three major processes occurring in the reaction mixture: the oxidation of AIMSAs (R3), the Dushman reaction<sup>27</sup> (R5), and the consumption of iodine (R6).



The different reaction profiles obtained are a result of the relative rates of these three processes. Reaction R5 is the reaction most dependent on acid concentrations and is responsible for the formation of iodine. In high acid environments it produces iodine at a faster rate than R6 can consume the iodine, and iodine accumulates. The depletion of the iodine after its formation is determined by the amount of AIMSAs.

**Formation of Iodine.** The data for the formation of iodine implicate a reaction which is first order in iodate and iodide and second order in acid. This suggests that the initial part of the reaction is dominated by the standard oxyhalogen reaction:<sup>27</sup>



followed by



where  $R \equiv -C(NH)NH_2$ .

Only catalytic amounts of  $I^-$  will be needed for reaction R7 to commence. The  $I^-$  used in R7 will be regenerated in the reduction of the oxyiodide species. The rate of reaction can be deduced from the following sequence:

$$\text{rate} = -d[AIMSAs]/dt = k_2[HOI][AIMSAs]$$

After substituting for HOI, one obtains the following rate equation:

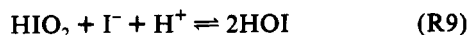
$$\text{rate} = \frac{-d[AIMSAs]}{dt} = \frac{k_1[IO_3^-][I^-][H^+]^2[AIMSAs]}{k_{-1}[HIO_2] + k_2[AIMSAs]} \quad (3)$$

At the beginning of the reaction, when  $[AIMSAs] \gg [HOI]$  and  $[HIO_2]$ ,  $HIO_2$  will be zero to negligible, and eq 3 becomes

$$\text{rate} = k^{app}[IO_3^-][I^-][H^+]^2 \quad (4)$$

where  $k^{app}$  is the apparent rate constant.

Our experimental data support eq 4. The iodide concentration increases during the course of the reaction. It enhances the reaction by forming more HOI from  $HIO_2$  through reaction R9.



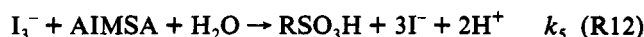
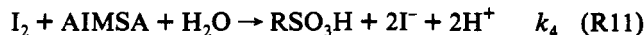
Iodine will then be formed by the HOI/ $I^-$  reaction (R10).



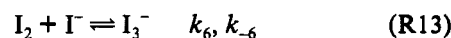
Although R10 is very fast, iodine will not accumulate until its rate of formation is greater than its rate of consumption. The rate of formation of iodine is related to the length of the induction period. A short induction period indicates that the rate of

formation of iodine is fast and that it quickly overwhelms its rate of consumption by AIMSAs. Our data, which show an inverse square dependence on  $[H^+]$  and inverse dependences on both  $[IO_3^-]$  and  $[I^-]$ , strongly suggest eq 4 as the differential rate law for the formation of iodine.

**Consumption of Iodine.** Iodine is consumed through its reaction with AIMSAs. The reaction's inhibition by both acid and iodide suggests the following reaction scheme in which  $I_2$ ,  $I_3^-$ , and HOI are all active:



The reactions R9, R11, and R12 are coupled together by the rapid equilibria R10 and R13:



$$\begin{aligned} \text{rate} &= -d[I_2]/dt = -d[AIMSAs]/dt \\ &= k_2[HOI][AIMSAs] + k_4[I_2][AIMSAs] + \\ &\quad k_5[I_3^-][AIMSAs] \end{aligned}$$

After substituting for HOI and  $I_3^-$ , we obtain eq 5

$$\text{rate} = [I_2][AIMSAs] \left( k_4 + \frac{k_2 k_{-3}}{k_2[AIMSAs] + k_3[I^-][H^+]} + \frac{k_5 k_6 [I^-]}{k_5[AIMSAs] + k_{-6}} \right) \quad (5)$$

The terms in the denominators with  $[AIMSAs]$  can be neglected to give eq 6:

$$\text{rate} = [I_2][AIMSAs] \left( a + \frac{b}{[I^-][H^+]} + c[I^-] \right) \quad (6)$$

where  $a = k_4$ ,  $b = k_2 k_{-3}/k_3$ , and  $c = k_5 k_6/k_{-6}$ .

The derived rate equation (6) implies inverse acid dependence kinetics as has been observed in our experimental data (Figure 6b). With both  $[I^-]$  and  $[H^+]$  as variables, it is not possible to obtain an analytical solution to eq 6. In the limit of high initial iodide concentrations, however, an inverse acid dependence plot should give a slope of  $Qk_2k_3/k_{-3}[I^-]$  and an intercept of  $Q(k_4 + [I^-]k_5k_6/k_{-6})$ , where  $Q = [I_2]_0[AIMSAs]_0$  after assuming  $[I^-]_t$  as constant. It is difficult to deduce the dependence of the reaction with respect to  $[I^-]$  since it will depend on the relative magnitudes of  $k_2$ ,  $k_4$ , and  $k_5$ . A single acid dependence plot, however, gives two equations (from intercept and slope), which is insufficient to allow the evaluation of the three kinetics parameters  $k_2$ ,  $k_4$ , and  $k_5$ . Two (or more) acid dependence plots at different  $[I^-]_0$  can be used to evaluate all three parameters and to check the value of  $k_2$  deduced in each plot. Our experimental data deduced the following values in units of  $M^{-1} s^{-1}$ :  $k_2 = 278 \pm 30$ ;  $k_4 = 13.8 \pm 3.5$ , and  $k_5 = 2.8 \pm 0.5$ .

The full proposed mechanism that involves all three steps is shown in Table II (reactions M1–M11). Reactions M1–M4 are standard oxyiodide reactions while reactions M6–M11 are the iodine–sulfur reactions.

**Reaction M1.** This is the first step in the oxidation of iodide by iodate. It is the well-known rate-determining step in the Dushman reaction and related reactions.<sup>28</sup> The iodide used in this reaction can be regenerated in reaction M6.

**TABLE II: Proposed Mechanism for the AIMSA-Iodate Reaction**

no.	reaction
M1	$\text{IO}_3^- + \text{I}^- + 2\text{H}^+ \rightleftharpoons \text{HIO}_2 + \text{HOI}$
M2	$\text{HIO}_2 + \text{I}^- + \text{H}^+ \rightleftharpoons 2\text{HOI}$
M3	$\text{HOI} + \text{I}^- + \text{H}^+ \rightleftharpoons \text{I}_2 + \text{H}_2\text{O}$
M4	$\text{IO}_3^- + \text{HOI} + \text{H}^+ \rightleftharpoons 2\text{HIO}_2$
M5	$\text{I}_2 + \text{I}^- \rightleftharpoons \text{I}_3^-$
M6	$\text{HOI} + \text{AIMSA} \rightleftharpoons \text{RSO}_3\text{H} + \text{H}^+ + \text{I}^-$
M7	$\text{HOI} + \text{RSO}_3\text{H} + \text{H}_2\text{O} \rightleftharpoons \text{SO}_4^{2-} + \text{CO}(\text{NH}_2)_2 + \text{I}^- + 3\text{H}^+$
M8	$\text{I}_2 + \text{AIMSA} + \text{H}_2\text{O} \rightleftharpoons \text{RSO}_3\text{H} + 2\text{I}^- + 2\text{H}^+$
M9	$\text{I}_2 + \text{RSO}_3\text{H} + 2\text{H}_2\text{O} \rightleftharpoons \text{SO}_4^{2-} + \text{CO}(\text{NH}_2)_2 + 2\text{I}^- + 4\text{H}^+$
M10	$\text{I}_3^- + \text{AIMSA} + \text{H}_2\text{O} \rightleftharpoons \text{RSO}_3\text{H} + 3\text{I}^- + 2\text{H}^+$
M11	$\text{IO}_3^- + \text{AIMSA} + \text{H}^+ \rightleftharpoons \text{HIO}_2 + \text{RSO}_3\text{H}$

**Reaction M2.** This is a rapid reversible reaction<sup>29</sup> which controls the concentration of  $\text{HIO}_2$ . It is very important in our mechanism since we assume that  $\text{HIO}_2$  is passive and that most of the oxidation proceeds via  $\text{HOI}$  and  $\text{I}_2$ .

**Reaction M3.** This reaction was studied by Eigen and Kustin<sup>30</sup> using relaxation techniques. We used the kinetics parameters they deduced for our computer simulations study. The forward reaction will be by far the fastest reaction in this proposed mechanism. It is responsible for the transient formation of iodine (in high acid) since it is faster than the reactions that consume iodine.

**Reaction M4.** We do not anticipate this to be a very significant reaction in this mechanism because reactions M3, M6, and M7 will consume most of the  $\text{HOI}$  as it is formed. It is important at the end of the reaction in excess  $\text{IO}_3^-$  conditions to maintain stoichiometric consistency.

**Reaction M5.** The formation of  $\text{I}_3^-$  has been very important in explaining the autoinhibition observed in the  $\text{I}_2$ -SCN<sup>-</sup> reaction.<sup>16</sup>  $\text{I}_3^-$  is a poor electrophile and is relatively unreactive as an oxidizing agent when compared to  $\text{I}_2$ . We took the equilibrium constant of its formation to be  $770 \text{ M}^{-1}$  in our mechanism.<sup>31</sup> This equilibrium will be very important in our mechanism since the formation of  $\text{I}_3^-$  would slow down the consumption of iodine and allow it to accumulate.

**Reaction M6.** We expect this to be a relatively rapid oxygen-transfer reaction. The  $\text{I}^-$  released in this step can be used in reactions M1, M2, and M3. We have also made this reaction irreversible. In the low pH conditions utilized for this study, only a small proportion of the iodine-containing species will exist as  $\text{HOI}$ .

**Reaction M7.** As with M6, this should also be a reasonably rapid process, but due to the stability of the sulfonic acid, this reaction is slower than M6 and does not represent a major oxidation pathway in this mechanism at these very low pH values. In other oxidations of thiourea and thiocyanate, this step, which represents a cleavage of the sulfur-carbon bond, has been erroneously considered to be quite fast.<sup>14</sup> It is an irreversible process because of what we anticipate to be a very high positive entropy change which accompanies the reaction. It is also ineffective as an oxidation route but is essential in generating iodide for reactions M1, M2, and M3.

**Reaction M8.** This represents direct oxidation of the sulfur compound by iodine. It is a two-step process that involves an oxidation followed by hydrolysis. From our experiments this reaction appears to be a slow process. An earlier study had pegged  $k_{\text{M8}}$  at  $0.20 \text{ M}^{-1} \text{ s}^{-1}$  through a computer simulation procedure.<sup>20</sup> Our experimental data suggest a value of  $13.8 \pm 3.5 \text{ M}^{-1} \text{ s}^{-1}$ . This is the value we used for our simulations. Reaction M8 will progressively shut itself down as the reaction proceeds due to the formation of  $\text{I}^-$  which converts  $\text{I}_2$  to  $\text{I}_3^-$  and retards the reaction.

**Reaction M9.** The sulfonic acid is quite stable, and thus we expect  $k_{\text{M9}}$  to be small. Previous workers<sup>20</sup> had suggested a value of  $0.10 \text{ M}^{-1} \text{ s}^{-1}$ .

**Reaction M10.** This reaction is very slow. Our separate experiments on this reaction have shown it to be extremely slow

**TABLE III: Rate Constants and Rate Laws Used in the Numerical Simulations**

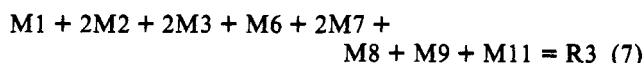
no.	$V$ (forward rate)	$V$ (reverse rate)
M1	$2.8[\text{IO}_3^-][\text{I}^-][\text{H}^+]^2$	$1.44 \times 10^3[\text{HIO}_2][\text{HOI}]$
M2	$2.1 \times 10^9[\text{HIO}_2][\text{H}^+][\text{I}^-]$	$9.0 \times 10^1[\text{HOI}]^2$
M3	$3.1 \times 10^{12}[\text{HOI}][\text{I}^-][\text{H}^+]$	$2.2[\text{I}_{2(\text{aq})}]$
M4	$8.6 \times 10^2[\text{IO}_3^-][\text{HOI}][\text{H}^+]$	$2.0[\text{HIO}_2]^2$
M5	$6.2 \times 10^9[\text{I}_2][\text{I}^-]$	$8.5 \times 10^6[\text{I}_3^-]$
M6	$2.78 \times 10^2[\text{HOI}][\text{AIMSA}]$	
M7	$4.0[\text{HOI}][\text{RSO}_3\text{H}]$	
M8	$1.38 \times 10^1[\text{I}_2][\text{AIMSA}]$	
M9	$2.0 \times 10^{-1}[\text{I}_2][\text{RSO}_3\text{H}]$	
M10	$2.8[\text{I}_3^-][\text{AIMSA}]$	
M11	$2.0[\text{IO}_3^-][\text{AIMSA}][\text{H}^+]$	

compared to M8 and M9 (see Figure 6a), and we used our experimentally-determined rate constant of  $2.8 \text{ M}^{-1} \text{ s}^{-1}$ .

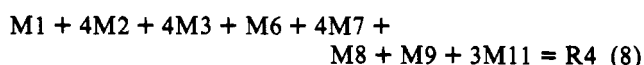
**Reaction M11.** This reaction basically initiates the reaction but is otherwise unimportant once the reaction has commenced.  $\text{HIO}_2$ , through reactions M2 and M6 (or M8), generates iodide which initiates reaction M1.

### Computer Simulations

The iodate-AIMSA reaction was simulated by using the 11-reaction 11-variable mechanism shown in Table II. The rate laws and rate constants used in the simulations are shown in Table III. The integrator used was the semi-implicit Runge-Kutta method devised by Kaps and Rentrop.<sup>32</sup> The simulations were simplified by the fact that we made reactions M6-M11 irreversible and that the kinetics parameters of the oxyiodide species reactions are mostly known. Of the 16 kinetics parameters needed in Table III to simulate this reaction, 13 are either known or were evaluated in this study, leaving only three parameters to be guessed ( $k_{\text{M7}}$ ,  $k_{\text{M9}}$ , and  $k_{\text{M11}}$ ). The stoichiometry of the reaction in excess AIMSA conditions can be derived from a sum of the following reaction steps:



The stoichiometry of the reaction in excess  $\text{IO}_3^-$  conditions is



Reactions M4 and M5 are not included in the stoichiometry because they are basic equilibria which control the concentrations of the halogen species, and M10 is not included because it is redundant in the overall stoichiometry; it results from rapid equilibrium R5. The stoichiometric coefficients in the stoichiometries were used as weighting factors in the simulations (from eqs 7 and 8).

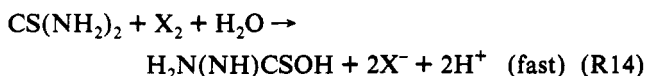
The simulations were most sensitive to  $k_{\text{M8}}$  and  $k_{\text{M11}}$ . The delicate balance between reactions M8 and M11 determined whether transient formation of iodine occurred in excess AIMSA as well as the position of the maximum iodine concentration. If one continuously reduced the value of  $k_{\text{M11}}$ , a value would be reached below which the simulations would no longer be sensitive to  $k_{\text{M11}}$ . At this point, reaction initiation would be occurring via M1 and the trace iodide concentrations that exist in all iodate solutions.<sup>26,33</sup>

The simulations were unsuccessful if composite of M6 + M7 and M8 + M9 were used instead of the individual reactions themselves. Though the simulations would still give the correct stoichiometric concentrations at the end of the reaction, they would fail to give the iodine concentration variations. The structure observed, as well, was heavily dependent on the prerequisite that the bimolecular reaction rates of the oxidation rates of the AIMSA to the sulfonic acid be faster than the corresponding oxidation rates of the sulfonic acid to the sulfate. Thus the sulfonic acid concentrations also showed a transient peak before going down to zero. The rate of disappearance of sulfonic acid was dependent on  $k_{\text{M7}}$  and  $k_{\text{M9}}$ . The low value of

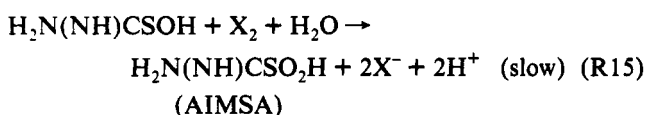
$k_{M10}$  (which we experimentally determined), coupled with the rapid equilibrium of reaction M5, justifies the iodide retardation observed in the oxidation of AIMSA by  $I_2$  (Figure 6a). In excess iodide concentrations over  $I_2$ , the major route of oxidation was still by  $I_2$  via the rapid exchange reaction M5. A very good fit was observed of the  $I_2$ -AIMSA reaction in the absence and presence of excess iodide. Figure 3 shows the comparison between experimental and simulated traces of iodine concentrations in excess  $IO_3^-$ .

## Discussion

The simple mechanism which we have presented seems to offer a consistent explanation for the kinetics data and the observed nonlinear reaction dynamics. Studies of the oxidation of thiourea by bromine and by aqueous iodine displayed a very rapid initial rate in which 1 mol of thiourea consumed 1 equiv of the oxidant to give the sulfenyl acid:<sup>15</sup>



where X can be I or Br. The rest of the reaction was much slower and rate-determining:



Due to the rapid autoxidation that takes place between the sulfenyl, sulfinic, and sulfonic acids, the last step in the mechanism is the formation of sulfate from the sulfonic acid. The only intermediate in the oxidation of AIMSA is the sulfonic acid,  $RSO_3H$ , which does not dimerize or react with AIMSA but may undergo a slow autoxidation process in the absence of further oxidizing agent. This sulfonic acid intermediate is very stable and can be isolated as a product.<sup>34</sup> The oxidation of thiourea by chlorine dioxide, for example, gives the sulfonic acid as the major product, and there is negligible oxidation of the sulfonic acid to sulfate.<sup>34</sup> The AIMSA- $IO_3^-$  reaction is a much simpler oxidation, as evidenced by the easily reproducible kinetics data as well as a very clean stoichiometric determination.

**Induction Period.** The initial velocities of all reactions,  $V_i = k_i[a_i]^n[b_i]^m \dots$ , are limited by the starting concentrations of their reactant species, some of which may not attain appreciable values until later in the reaction, e.g., reactions M1, M2, M3, M5, and M6. In the initial stages the reactions form  $HIO_2$  and  $HOI$  (M1, M11). Through reactions  $M2 + M5 + M6$  iodide is built up in the system. Addition of reactions  $M1 + M2 + M5$  shows that 2 mol of  $I^-$  yields 3 mol of  $I^-$ . The  $I^-$  formed can participate in reaction M1 or combine with  $HOI$  to give  $I_{2(aq)}$ . The rate of formation of iodine in our reaction system is given by

$$d[I_2]/dt = V_{M3} - (V_{M5}) - V_{M8} - V_{M9} \quad (R16)$$

$V_{M5}$  is in parentheses because the experiments were performed at the isosbestic point of  $I_2/I_3^-$ ; formation of  $I_3^-$  will not be noticed by the spectrophotometer. The end of the induction period is when  $V_{M3} > V_{M8} + V_{M9}$ . If the  $[AIMSA]_0$  is high, then  $V_{M8} + V_{M9}$  will be high enough and greater than  $V_{M3}$ , and iodine will not accumulate. An induction period will not exist. This behavior has been observed in our experiments. The induction period in our mechanism is thus the period from  $t = 0$  to  $t$  when  $V_{M3} > V_{M8} + V_{M9}$ .

**Acid Dependence.** Acid has been quite pivotal in determining the observed reaction dynamics. Acid concentration controls a number of features: (1) in very low acid concentrations and excess AIMSA no  $I_2$  is formed, although the oxidation of AIMSA will still proceed to completion; (2) in excess  $IO_3^-$  and low acid concentrations, we observe an induction period followed by a slow monotonic increase in  $I_2$  concentration with no  $I_2$  transient

peak; and (3) the length of the induction period is inversely proportional to  $[H^+]^2$ . These observations show that acid strongly catalyzes the reaction that forms iodine and either does not catalyze or retards the reactions that consume  $I_2$ . In this case acid retards  $I_2$  consumption. These features (a-c) can thus all be traced to reaction M1 in our mechanism. Reaction M1 is the most important in terms of determining length of induction period.  $V_{M1} = k_{M1}[IO_3^-][I^-][H^+]^2$  is strongly acid dependent, while  $V_{M6} + V_{M7} + V_{M8} + V_{M9} + V_{M10}$  contain both acid-independent and acid-inhibited terms. In high acid concentrations,  $V_{M1}$ ,  $V_{M2}$ , and  $V_{M3}$  are all fast (formation of iodine), while  $V_{M6}$ - $V_{M10}$  (consumption of iodine) are retarded by acid.

**Other Features.** Variation of  $[IO_3^-]_0$  at constant  $[H^+]_0$  and  $[AIMSA]_0$  gave the traces shown in Figure 5. Due to the high  $[H^+]_0$ , in all the traces shown in this figure  $I_2$  is formed. At low  $[IO_3^-]_0$  all  $I_2$  formed is consumed by the end of the reaction. Finite iodine concentration at the end of the reaction can only be obtained if stoichiometry R3 is satisfied. As soon as the stoichiometry is satisfied, the excess  $IO_3^-$  will react with the  $I^-$  in the product and form  $I_2$ . Our model can correctly predict this behavior.

**Acknowledgment.** We acknowledge helpful discussions with Cordelia Chinake. This work was funded by the West Virginia EPSCoR program.

## References and Notes

- (1) Part 1 in the series Nonlinear Dynamics in Chemistry Derived From Sulfur Chemistry.
- (2) For a listing of a number of oxychlorine-sulfur oscillators, see: Orban, M.; Epstein, I. R. *J. Am. Chem. Soc.* **1982**, *104*, 5911.
- (3) Orban, M.; Epstein, I. R. *J. Am. Chem. Soc.* **1985**, *107*, 2302.
- (4) Vesilind, P. A.; Peirce, J. J. *Environmental Pollution and Control*, 2nd ed.; Butterworths: Boston, 1983.
- (5) Alamgir, M.; Epstein, I. R. *Int. J. Chem. Kinet.* **1985**, *17*, 429.
- (6) Rabai, G.; Beck, M.; Kustin, K.; Epstein, I. R. *J. Phys. Chem.* **1989**, *93*, 2853.
- (7) Edblom, E.; Luo, Y.; Orban, M.; Kustin, K.; Epstein, I. R. *J. Phys. Chem.* **1989**, *93*, 2722.
- (8) Orban, M.; Epstein, I. R. *J. Am. Chem. Soc.* **1987**, *109*, 101.
- (9) Nagypal, I.; Epstein, I. R.; Kustin, K. *Int. J. Chem. Kinet.* **1986**, *18*, 345.
- (10) Nagypal, I.; Bazsa, G.; Epstein, I. R. *J. Am. Chem. Soc.* **1986**, *108*, 3635.
- (11) Chinake, C.; Simoyi, R. H., manuscript in preparation.
- (12) Ouyang, Q.; De Kepper, P. *J. Phys. Chem.* **1987**, *91*, 6040.
- (13) We have performed kinetics studies mainly on thiourea and thiocyanate because they are involved in clock reactions and in chemical oscillations. See refs 14-16.
- (14) Epstein, I. R.; Kustin, K.; Simoyi, R. H. *J. Phys. Chem.* **1992**, *96*, 5852.
- (15) Simoyi, R. H.; Epstein, I. R. *J. Phys. Chem.* **1987**, *91*, 5124.
- (16) Simoyi, R. H.; Epstein, I. R.; Kustin, K. *J. Phys. Chem.* **1989**, *93*, 2792.
- (17) Luo, Y.; Orban, M.; Kustin, K.; Epstein, I. R. *J. Am. Chem. Soc.* **1989**, *111*, 4541.
- (18) Hashimoto, S.; Sunamoto, J. *Bull. Chem. Soc. Jpn.* **1966**, *39*, 1207.
- (19) Barnard, D. *J. Chem. Soc.* **1957**, 4675.
- (20) Rabai, G.; Beck, M. *J. Chem. Soc., Dalton Trans.* **1985**, 1669.
- (21) Simoyi, R. H. *J. Phys. Chem.* **1986**, *90*, 2802.
- (22) Rabai, G.; Orban, M.; Epstein, I. R. *Acc. Chem. Res.* **1990**, *23*, 258.
- (23) Kice, J. L.; Cleveland, J. P. *J. Am. Chem. Soc.* **1973**, *95*, 104.
- (24) Rabai, G.; Wang, R. T.; Kustin, K. *Int. J. Chem. Kinet.* **1992**, *25*, 53.
- (25) Boltz, F. D.; Howell, J. A. (Eds.) *Colorimetric Determination of Nonmetals*; Wiley and Sons: New York, 1978; p 186.
- (26) King, D. E. C.; Lister, W. M. *Can. J. Chem.* **1968**, *46*, 279.
- (27) Dushman, S. *J. Phys. Chem.* **1904**, *8*, 453.
- (28) Abel, E.; Stadler, F. Z. *Phys. Chem.* **1926**, *122*, 49.
- (29) Faria, R. de B.; Lengyel, I.; Epstein, I. R.; Kustin, K. *J. Phys. Chem.* **1993**, *97*, 1164.
- (30) Eigen, M.; Kustin, K. *J. Am. Chem. Soc.* **1962**, *84*, 1355.
- (31) Turner, D. H.; Flynn, G. W.; Sutin, N.; Beitz, J. V. *J. Am. Chem. Soc.* **1972**, *94*, 1554.
- (32) Kaps, P.; Rentrop, P. *Numer. Math.* **1979**, *23*, 55.
- (33) Simoyi, R. H., manuscript in preparation.
- (34) Rabai, G.; Wang, R. T.; Kustin, K. *Int. J. Chem. Kinet.* **1992**, *25*, 53.